

Thermal Analysis of an Antenna

Kuiyuan Shen, Guangyu Wang, Quan Wen

School of Mechanical Engineering, Nanjing University of Science and Technology, Nanjing, China

Email: 1015424301@qq.com

How to cite this paper: Shen, K.Y., Wang, G.Y. and Wen, Q. (2022) Thermal Analysis of an Antenna. *Journal of Applied Mathematics and Physics*, 10, 2574-2580.

<https://doi.org/10.4236/jamp.2022.108174>

Received: July 28, 2022

Accepted: August 28, 2022

Published: August 31, 2022

Abstract

In order to study the internal temperature changes and heat transfer phenomena of a model during external warming, a heat transfer simulation was conducted. The thermal analysis of the model was simulated by using ANSYS/LS-DYNA software, and the heat and heat transfer phenomena of the warhead in the actual process were simulated by setting the temperature conditions on the surface of the model, and the model boundary and internal temperature changes were obtained from the simulation experiments, and relevant conclusions were drawn.

Keywords

Thermal Analysis Simulation, Heat Transfer

1. Introduction

At present, with the continuous development of computer hardware facilities, the calculation and analysis speed of computers has been rapidly increased. Because of the difficulty and high cost of testing heat conduction experiments in the actual process [1], computer simulation is usually used to simulate the experiments before the actual experiments, and the improvement of computer hardware performance nowadays makes the simulation more accurate and detailed [2].

This experiment is an experimental simulation of data from a thermal analysis experiment conducted on a model of the head of a projectile. Considering the complexity of the actual heat transfer situation, ANSYS/LS-DYNA [3] is used as the simulation software.

2. Simulation Experiment Preparation

2.1. Geometric Modeling

Before the simulation analysis, the geometric model of the device needs to be es-

established, including the geometric models of the radome, heat shield, thermal protection layer, antenna, metal connection ring and other components, as shown in **Figure 1**. Since the structure of the device has axisymmetric characteristics, only its axisymmetric cross section is needed to build the geometric model [4], and the three-dimensional model is simplified to a two-dimensional plane model in order to reduce the calculation. The software used to build the geometric model is Solidworks [5], which has a good fit with ANSYS/LS-DYNA.

2.2. Delineating the Finite Element Mesh

Import the geometric model from the previous step into the meshing software. The finite element meshing is performed for the geometric characteristics of the simulation object. For the above device, its structure and thermal boundary conditions have axisymmetric characteristics, so the heat conduction process in the device can be considered as an axisymmetric problem [6], and the model cross-section is meshed using planar quadrilateral cells [7], as shown in **Figure 2**. This can greatly reduce the simulation calculation volume and speed up the simulation analysis.



Figure 1. Example of a figure caption (figure caption).

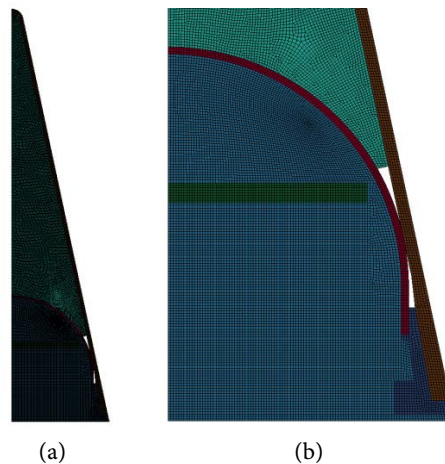


Figure 2. A device finite element model meshing. (a) Overall meshing of the finite element model; (b) local meshing of the finite element model.

2.3. Simulation Model of Heat Transfer Process inside a Device

The delineated finite element mesh is imported into LS-PrePost, the pre-processing software of ANSYS/LS-DYNA, and keywords are added to establish a complete heat transfer simulation model. The model of a device after importing LS-PrePost is shown in **Figure 3**.

In order to reduce the computational effort and speed up the computer simulation, the cell type used for this heat transfer analysis is a planar quadrilateral cell.

Firstly, material models were added to the air domain (density of 1.29 kg/m^3) in LS-PrePost as listed in **Table 1**; secondly, material models were added to the radome; then, material models were added to the heat shield; next, material models [8] were added to the thermal shield, Yin steel ring, and antenna (**Table 2**).

The initial temperature of the model is 313 K (39.85°C). Add thermal boundary conditions to the model [9], as shown in **Figure 4**.

Table 1. Air thermal physical model parameters.

Temperature (K)	Air	
	Specific heat (J/(kg·K))	Thermal conductivity
293.15 K	717.70	0.0259
460.96 K	736.23	0.0375
628.77 K	770.89	0.0476
796.58 K	810.88	0.0570
964.38 K	845.97	0.0659
1132.19 K	875.74	0.0742
1300.00 K	897.30	0.0824

Table 2. Thermophysical parameters of model materials.

Parameters	Antenna Cover	Heat shield	Thermal protection layer	Metal connecting ring	Bonding agent
Materials	SCFC	Silicon dioxide based porous materials	Silicone based materials	Invar	High temperature bonding agent
Density (kg/m^3)	1950	$0.3 \times 10^3 - 0.4 \times 10^3$	$0.9 \times 10^3 - 1.2 \times 10^3$	8.1×10^3	1.1×10^3
Thermal conductivity (W/mK)	0.78 (25°C) 0.91 (300°C) 1.25 (800°C)	0.06 (25°C) 0.1 (600°C)	0.2 - 0.5	10 - 13	0.2 - 0.3
Specific heat (J/kg·K)	756 (25°C) 1008 (300°C) 1176 (800°C)	630 - 700	1100 - 1200	515	1740

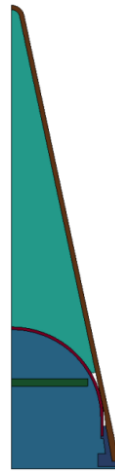


Figure 3. Model of a device after importing LS-PrePost.

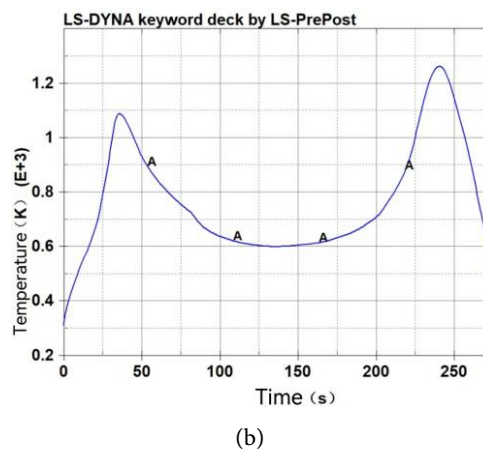
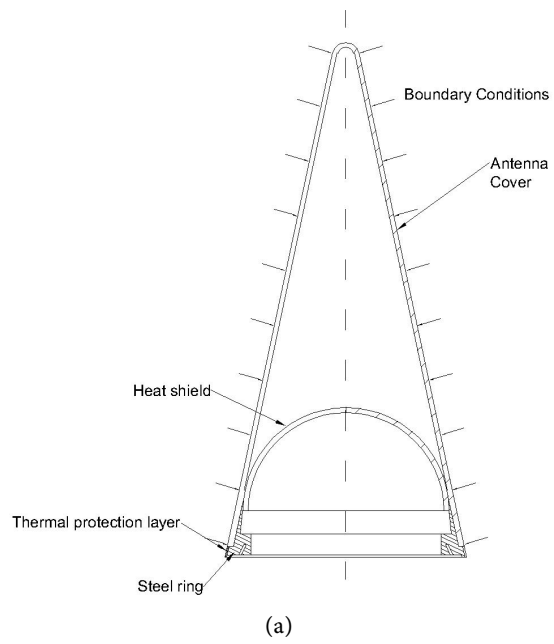


Figure 4. Model thermal boundary condition setting. (a) Model thermal boundary conditions; (b) thermal boundary conditions temperature change curve.

Set other parameters required for thermal simulation analysis in LS-PrePost, such as thermal conductivity between components, simulation step size, solver parameters, etc.

3. Simulation Experiment Results

By conducting thermal analysis simulation experiments on the model, the internal temperature distribution states of the model at different moments are obtained [10]. To ensure the uniformity and continuity of the overall simulation state, the temperature distribution clouds at five time points of 50 s, 100 s, 150 s, 200 s, and 250 s are intercepted by using the equal difference time division. As shown in **Figure 5**.

After analyzing the temperature distribution at each time point of the model, the temperature of the inner surface of the top of the heat shield [11] and the maximum temperature of the antenna were calculated to obtain the following **Figure 6** and **Figure 7**.

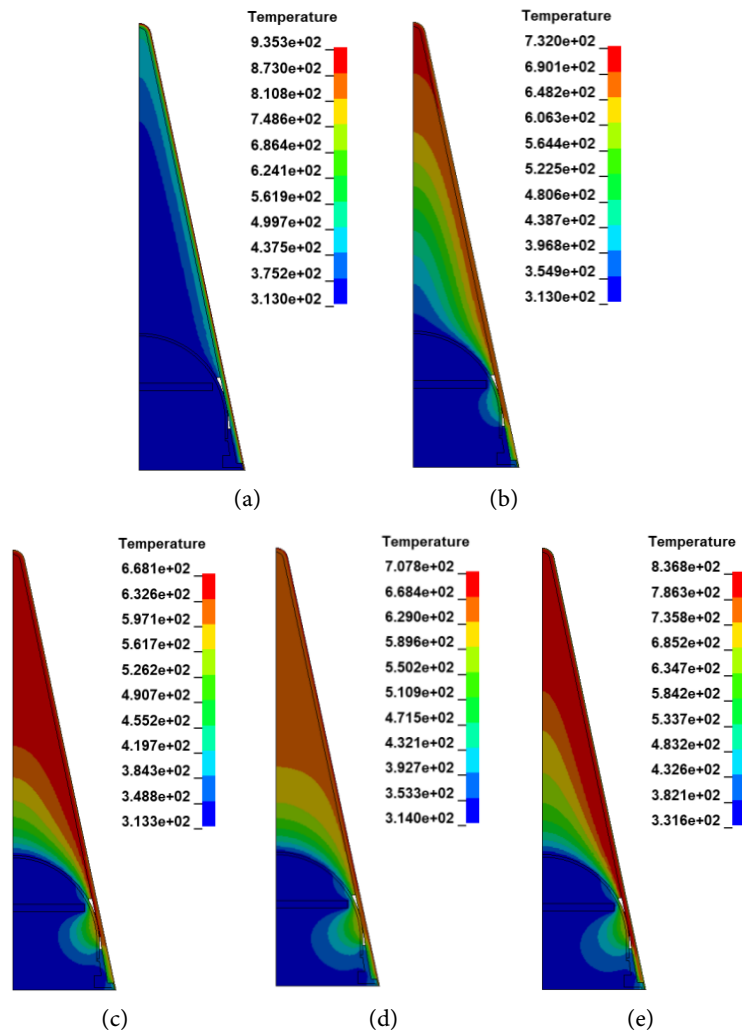


Figure 5. Cloud diagram of the internal temperature distribution of a device at different moments. (a) 50 s; (b) 100 s; (c) 150 s; (d) 200 s; (e) 274 s.

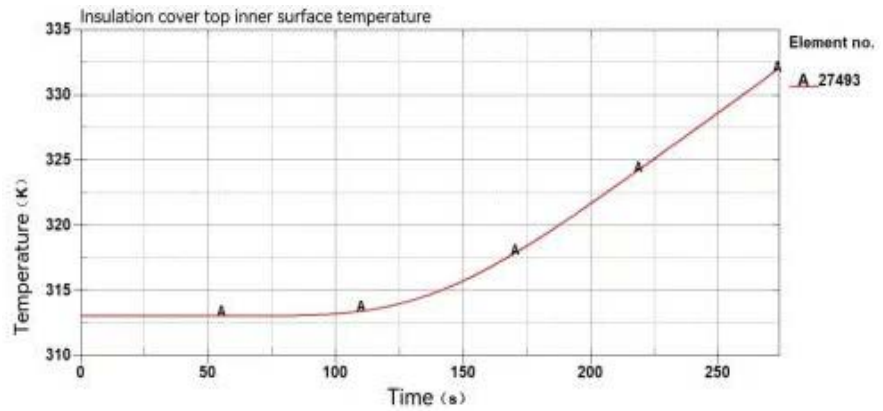


Figure 6. Temperature variation of the inner surface of the top of the heat shield.

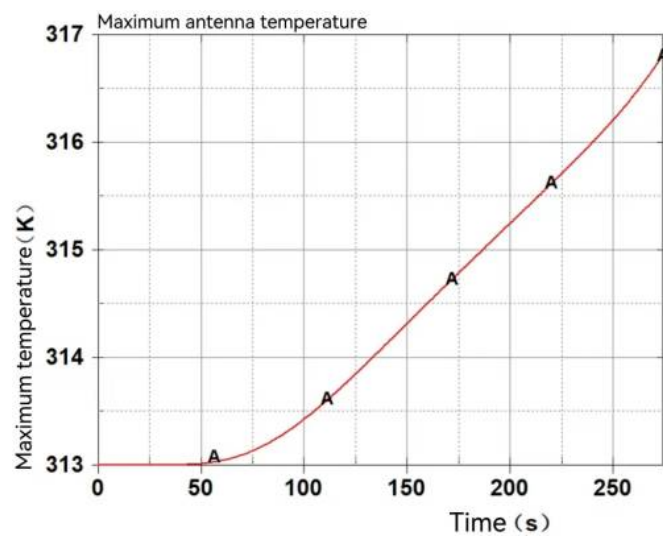


Figure 7. Variation of maximum antenna temperature.

4. Experimental Conclusion

1) After the thermal analysis of the warhead model, we found that the temperature difference between the exterior and interior of the heat shield is very obvious, before 100 s, the heat shield and the internal temperature remain basically unchanged, and after 100 s, the temperature gradually increases and the rate of temperature rise remains basically unchanged, with a high degree of linearity of temperature change.

2) The maximum temperature of the antenna is maintained at about 313 K before 50 s, and it starts to warm up after 50 s with a high degree of linearity of the temperature rise curve.

3) During the experiment, the temperature transfer between the model shell to the internal heat shield showed a clear stratification, the closer the location to the surface of the projectile the faster the rate of heat transfer, and conversely, the closer the location to the heat shield the slower the heat transfer rate of the part.

Conflicts of Interest

The authors declare no conflicts of interest regarding the publication of this paper.

References

- [1] Zhuang, Z., Hu, M., Wang, Y.N., Dai, R., Li, Q.L., Zhou, X.F., Wei, Y.Z. and Yang, L. (2017) ANSYS-Based Simulation Study on Heat Conduction of Dual-Frequency Microchip Lasers. *Optical Communication Technology*, **41**, 42-45.
- [2] Heat Transfer Research (2020) Findings from University of Alberta Yields New Findings on Heat Transfer Research (Nonlocal Dual-phase-lag Heat Conduction and the Associated Nonlocal Thermal-viscoelastic Analysis). *Journal of Technology*.
- [3] Wei, L.H. (2009) Mathematical Modeling of Quenching Heat Conduction and Its Finite Element Simulation Analysis. *Mining Machinery*, **37**, 38-41.
- [4] Zhang, C., Zhang, S. and Xue, J.Y. (2013) Boundary Element-Based Simulation of Transient Heat Transfer in Functional Gradient Materials. *Computer Simulation*, **30**, 25-29.
- [5] Zhang, X.L., Wang, C., Zhou, M.R., Ji, C.M. and Wang, X.D. (2020) Heat Conduction Test and Simulation Analysis of Asphalt Concrete Pavement Scarification. *Subgrade Engineering*, 58-62.
- [6] Cao, L.L., Pei, J.Z., Zhang, X.M. and Liu, Q. (2012) Simulation of Heat Conduction Problems in Functional Gradient Materials. *Computer Simulation*, **29**, 387-390.
- [7] Luo, J.B., Huang, Y., Li, J., Wang, G. and Zhang, W.X. (2019) Simulation Study of High-Pressure Forming within Asymmetric Pipe Fittings. *Journal of Guangxi University of Science and Technology*, **30**, 30-35.
- [8] da Silva, W.B., Dutra, J.C.S., Kopperschimdt, C.E.P., Lesnic, D. and Aykroyd, R.G. (2021) Sequential Particle Filter Estimation of a Time-Dependent Heat Transfer Coefficient in a Multidimensional Nonlinear Inverse Heat Conduction Problem. *Applied Mathematical Modelling*, 89.
- [9] Chaudhari, K.K. and Sutar, C.S. (2021) Effect of Convection Boundary Condition on Hyperbolic Heat Conduction in Thermoelastic Medium. *Journal of Mathematical and Computational Science*, **11**.
- [10] Yan, C.Z., Yang, Y. and Wang, G. (2021) A New 2D Continuous-Discontinuous Heat Conduction Model for Modeling Heat Transfer and Thermal Cracking in Quasi-Brittle Materials. *Computers and Geotechnics*.
- [11] Nolasco Serna, C., Afanador Garcia, N. and Guerrero Gómez, G. (2021) Comparison of Analytical Methods and Numerical Methods in Modeling the Physical Phenomenon of Heat Conduction with Free Radiation. *Journal of Physics: Conference Series*, **2102**.